

UC Davis

UC Davis Previously Published Works

Title

Identification of *Collimonas* gene loci involved in the biosynthesis of a diffusible secondary metabolite with broad-spectrum antifungal activity and plant-protective properties

Permalink

<https://escholarship.org/uc/item/1fm0t883>

Journal

Microbial Biotechnology, 14(4)

ISSN

1751-7907

Authors

Akum, Fidele N
Kumar, Ravi
Lai, Gary
et al.

Publication Date


2021-07-01

DOI

10.1111/1751-7915.13716

Peer reviewed

Identification of *Collimonas* gene loci involved in the biosynthesis of a diffusible secondary metabolite with broad-spectrum antifungal activity and plant-protective properties

Fidele N. Akum,¹ Ravi Kumar,² Gary Lai,² Catherine H. Williams,¹ Hung K. Doan¹ and Johan H.J. Leveau¹ 

¹Department of Plant Pathology, University of California Davis, Davis, CA, USA.

²Novozymes Inc, 1445 Drew Avenue, Davis, CA, USA.

Summary

In greenhouse and field trials, a bacterial mixture of *Collimonas arenae* Cal35 and *Bacillus velezensis* FZB42, but not Cal35 alone or FZB42 alone, was able to protect tomato plants from challenge with the soil-borne fungal pathogen *Fusarium oxysporum* f.sp. *lycopersici* (Fol). To identify genes and mechanisms underlying this property in Cal35, we screened a random transposon insertion library for loss of function and identified two mutants that were impaired completely or partially in their ability to halt the growth of a wide range of fungal species. In mutant 46A06, the transposon insertion was located in a biosynthetic gene cluster that was predicted to code for a hybrid polyketide synthase–non-ribosomal peptide synthetase, while mutant 60C09 was impacted in a gene cluster for the synthesis and secretion of sugar repeat units. Our data are consistent with a model in which both gene clusters are necessary for the production of an antifungal compound we refer to as carenaemins. We also show that the ability to produce carenaemin contributed significantly to the observed synergy between Cal35 and FZB42 in protecting tomato plants from Fol. We discuss the potential for supplementing *Bacillus*-based

biocontrol products with *Collimonas* bacteria to boost efficacy of such products.

Introduction

The ability to suppress fungal growth is a common characteristic among members of the bacterial genus *Collimonas* (Leveau *et al.*, 2010). For its best known and studied representative, *Collimonas fungivorans* Ter331 (CfTer331), two sets of genes that contribute to antifungal activity have been described. One is the NLP gene that codes for a non-ribosomal peptide synthetase (NRPS) and directs the biosynthesis of a lipopeptide with a predicted Leu-Thr-X-Ser-Ile peptide core attached to a fatty acid side-chain and with *in vitro* efficacy against the plant pathogenic fungi *Fusarium culmorum* and *Rhizoctonia solani* (Song *et al.*, 2015). The other is the *colABC-DEFG* gene cluster (Kai *et al.*, 2018), which is located on a chromosomal locus called cluster K (Fritsche *et al.*, 2014) and codes for the biosynthesis of polyacetylenic compounds referred to as collimomycins (Fritsche *et al.*, 2014) or collimonins (Kai *et al.*, 2018). These compounds feature an ene–triyne moiety that is essential for antifungal activity (Kai *et al.*, 2018) and is formed through the combined action of the polyketide synthase (PKS) ColA and the desaturases ColB, ColC and ColD (Fritsche *et al.*, 2014; Kai *et al.*, 2018). In confrontation with laboratory strains of the fungus *Aspergillus niger*, collimomycin-producing CfTer331 induces the stunting, swelling, branching and pigmentation of hyphae (Fritsche *et al.*, 2014; Kai *et al.*, 2018) and interrupts the process of spore germination (Mosquera *et al.*, 2020). Not all *Collimonas* strains for which fungal suppression has been demonstrated carry the NLP gene or gene cluster K (Mela *et al.*, 2012; Fritsche *et al.*, 2014; Song *et al.*, 2015), suggesting the existence of much unexplored genetic potential for antifungal activity in the *Collimonas* pangenome.

The fungistatic properties of collimonads have sparked interest in their use as biocontrol agents for the management of fungal diseases of plants. CfTer331 was shown to protect tomato plants from the soilborne fungal pathogen *Fusarium oxysporum* f.sp. *radicis-lycopersici*, which

Received 19 September, 2020; revised 6 November, 2020; accepted 9 November, 2020.

For correspondence: E-mail jlleveau@ucdavis.edu; Tel. +1 530 752 5046; Fax: +1 530 752 5674.

Microbial Biotechnology (2021) 14(4), 1367–1384

doi:10.1111/1751-7915.13716

Funding Information Research reported here was supported by Novozymes North America, Inc. JHJL and HKD are both listed as inventors on patent # US 9,485,994 B2 (issued 8 November 2016) which is entitled 'Synergy-based biocontrol of plant pathogens' and based on previously published work on *Collimonas*-*Bacillus*-based suppression of plant disease (Doan *et al.*, 2020).

© 2020 The Authors. *Microbial Biotechnology* published by John Wiley & Sons Ltd and Society for Applied Microbiology.

This is an open access article under the terms of the Creative Commons Attribution-NonCommercial-NoDerivs License, which permits use and distribution in any medium, provided the original work is properly cited, the use is non-commercial and no modifications or adaptations are made.

causes tomato foot and root rot (Kamilova *et al.*, 2007). Whether this protection is linked to the production of collimomycin or the NLP-encoded lipopeptide remains unknown. Recently, another *Collimonas* isolate, *C. arenae* Cal35 (*CaCal35*), was shown to protect tomato plants from the root pathogen *Fusarium oxysporum* f. sp. *lycopersici* (*Fol*), the causal agent of Fusarium wilt (Doan *et al.*, 2020). However, it did so only when mixed together with Serenade Soil, a commercially available biocontrol product that features *Bacillus velezensis* (formerly *subtilis*) strain QST713 (*BvQST713*) as its active ingredient. Neither *CaCal35* by itself nor Serenade Soil by itself was able to mitigate the formation of symptoms that are typical of Fusarium wilt and include vascular discoloration and reduced shoot weight (Doan *et al.*, 2020). The mechanism underlying this emerging property of 'biocombicontrol' (Doan *et al.*, 2020) by the *CaCal35*-*BvQST713* mixture is not known. *BvQST713* has been shown to synthesize and secrete a suite of lipopeptides, including iturin, agrastatin/plipastatin and surfactin, which cause inhibition of spores and germ tubes (Marrone, 2002; Manker, 2004). No such secondary metabolites have yet been ascribed to *CaCal35*, which in laboratory assays outperformed all other tested *Collimonas* strains, including Ter331, in terms of overall fungal target range and growth suppression (Doan *et al.*, 2020). *CaCal35* does not possess a gene cluster K (Wu *et al.*, 2015), which rules out a role for collimomycin.

The goal of the study reported here was to identify and characterize the genes that underlie the antifungal activity of *CaCal35* and to determine if these genes contribute to biocombicontrol together with *Bacillus* bacteria. Instead of *BvQST713*-based Serenade Soil, we opted to use another well-studied biocontrol strain called *B. velezensis* FZB42 (*BvFZB42*) (Borriss, 2011). Formerly known as *Bacillus amyloliquefaciens* subsp. *plantarum* FZB42 (Borriss, 2011; Chowdhury *et al.*, 2015a; Dunlap *et al.*, 2016; Fan *et al.*, 2018), this bacterium suppresses the growth of many plant pathogenic fungi *in vitro* and protects crop plants such as cotton, tomato and lettuce against various plant pathogens (Yao *et al.*, 2006; Gül *et al.*, 2008; Chowdhury *et al.*, 2013; Chowdhury *et al.*, 2015b). Much like *BvQST713*, *BvFZB42* produces lipopeptides with antifungal properties, including bacillomycin D (an iturin), fengycin (related to plipastatin) and surfactin (Chen *et al.*, 2007; Chowdhury *et al.*, 2015a). The *BvFZB42* double-mutant AK3, which is unable to produce bacillomycin D as well as fengycin, is severely impaired in its ability to inhibit fungal growth (Koumoutsis *et al.*, 2004).

We show here that the ability of *CaCal35* to suppress *in vitro* the hyphal growth of previously tested and untested fungi, including *A. niger* and *Fol*, is correlated with the production of a diffusible activity that we refer to

as carenaemin. Screening of a *CaCal35* transposon insertion library for loss-of-function mutants led us to two chromosomal loci with a purported role in carenaemin production. The genetic and molecular characterization of these loci allowed us to propose a model for the PKS/NRPS-dependent synthesis of carenaemin and for the way in which carenaemin contributes to the reduction of *Fol*-induced symptoms on tomato plants by a mixture of *CaCal35* and *BvFZB42*.

Results

Broad-spectrum, diffusible antifungal activity produced by CaCal35

In no-contact confrontation assays on PDA plates, *CaCal35* inhibited colony expansion of *A. niger*, *Fusarium oxysporum* f.sp. *lycopersici* (*Fol*), *F. oxysporum* f.sp. *fragariae* (*Fof*), *Rhizoctonia solani*, *Sclerotium rolfsii*, *Sclerotinia sclerotiorum*, *Verticillium dahliae* and *Magnaporthe grisea* (Fig. 1, panels A2-H2), compared to control plates (fungus only, Fig. 1, panels A1-H1). For *A. niger*, this antifungal activity of *CaCal35* (Fig. 2B, compared to 2A, fungus only) was shown to be diffusible and expressed in the absence of fungus, as follows. After culturing *CaCal35* in the presence (Fig. 2B) or absence (Fig. 2D) of *A. niger* on PDA agar plates for 3 days, the sections of agar containing bacteria and fungi were removed using a sterile surgical blade. The remaining sections of agar were inoculated with *A. niger* spores at different distances relative to where *CaCal35* had been growing on the plate. Compared to the control (Fig. 2A), *A. niger* was unable to grow on agar on which *CaCal35* had been previously and proximally grown in the presence of *A. niger* (Fig. 2C), suggesting that the antifungal activity of *CaCal35* was water-soluble and diffusible through agar. We also observed that growth of *A. niger* was inhibited on agar on which *CaCal35* had been previously grown in the absence of *A. niger* and that the degree of inhibition decreased as a function of the distance between *A. niger* and *CaCal35* (Fig. 2E-G). This observation is consistent with diffusion and dilution of the antifungal activity away from its source, *CaCal35*. We postulate that this antifungal activity represents a secondary metabolite that will be referred to hereafter as carenaemin.

Biocontrol of tomato Fusarium wilt by CaCal35 in combination with BvFZB42

Notwithstanding the observed antifungal activity of *CaCal35* against *Fol* on agar plates (Fig. 1, panel B2), greenhouse-grown tomato plants were not protected from *Fol*-induced loss of biomass (Fig. 3A) or vascular discoloration (Fig. 3B) by prior root inoculation with

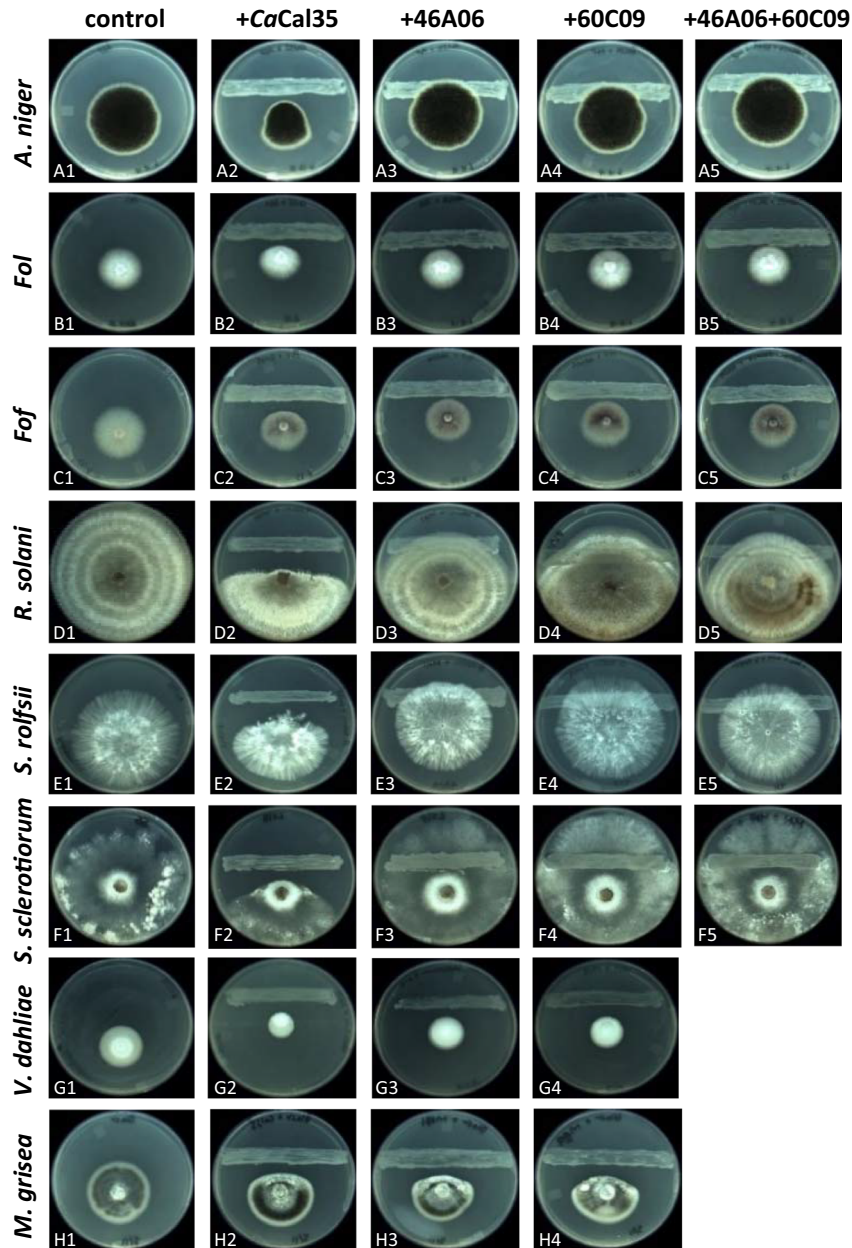


Fig. 1. Photographs showing hyphal growth of *A. niger*, *Fol*, *Fof*, *R. solani*, *S. rolfsii*, *S. sclerotiorum*, *V. dahliae* and *M. grisea* on PDA plates in the absence or presence of *CaCal35* or its transposon insertion mutants 46A06 and/or 60C09. Five microlitres of a suspension of 10^5 fungal spores/ml in water (*A. niger*, *Fol*, or *V. dahliae*), agar plugs (*Fof*, *R. solani*, *S. sclerotiorum*, *M. grisea*) or single matured sclerotia (*S. rolfsii*) was inoculated onto PDA plates that were either not inoculated with bacteria (first column) or line-inoculated at a 2 cm distance from the spores with *CaCal35* (second column), mutant 46A06 (third column), mutant 60C09 (fourth column) or a 1:1 mixture of 46A06 and 60C09 (fifth column). Plates were incubated at 28°C. Photographs were taken 5 days (*A. niger*, *S. rolfsii*), 4 days (*Fol*, *Fof*) or 7 days (*R. solani*, *S. sclerotiorum*, *M. grisea* and *V. dahliae*) after the plates were inoculated. The 46A06/60C09 mixture was not tested against *V. dahliae* or *M. grisea*.

CaCal35. Under the same conditions, *BvFZB42* did not protect tomato plants from *Fol* either (Fig. 3A and B). However, when mixed together, *CaCal35* and *BvFZB42* (referred to as '*Colli42*') significantly reduced ($P < 0.05$) *Fol*-induced loss of biomass (Fig. 3A) as well as vascular discoloration (Fig. 3B). *Fol*-challenged plants that were *Colli42*-treated looked like unchallenged (i.e. no-

Fol) plants (Fig. S1D and A, respectively), whereas *Fol*-challenged plants that were treated with *CaCal35* or *BvFZB42* looked like untreated *Fol*-challenged plants (Fig. S1C, E, and B respectively).

Protection by *Colli42* was also observed in an experimental *Fol*-infested field of tomato plants: only the *Colli42* treatment significantly ($P < 0.05$) reduced *Fol*-

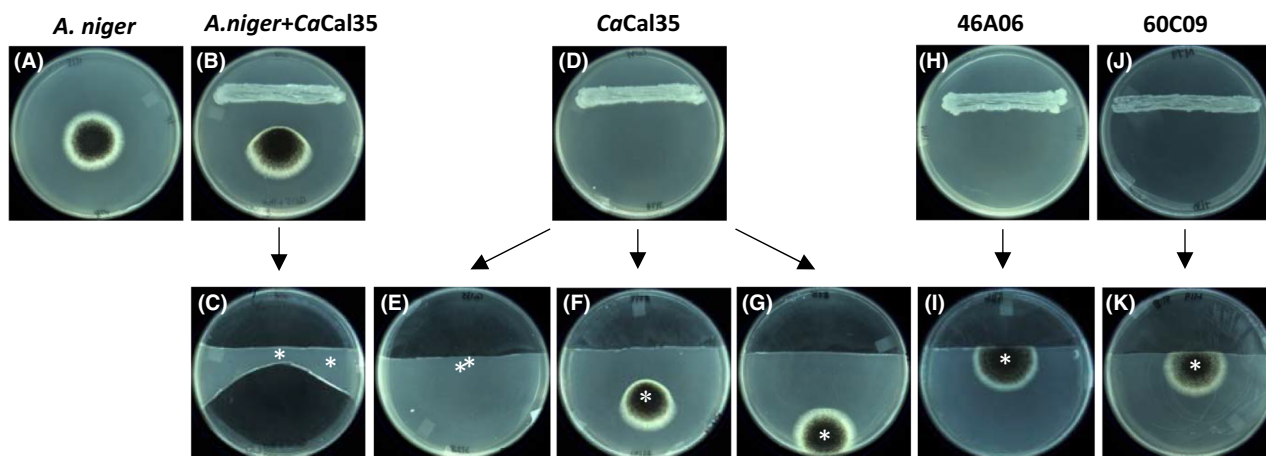


Fig. 2. Expression of antifungal activity by *CaCal35* in the presence or absence of *A. niger* and comparison to transposon insertion mutants 46A06 and 60C09. For this experiment, *CaCal35*, 46A06 or 60C09 was line-inoculated onto PDA in the presence (*CaCal35* only) or absence (*CaCal35*, 46A06, 60C09) of *A. niger* and incubated at 28°C (photographs B, D, H and J). After the removal of agar sections containing bacteria and/or fungi, the agar was spot-inoculated with 5 µl of a 10⁵ spore/ml spore suspension of *A. niger* at different distances (approximately 1.5, 3 or 4.5 cm) from where *CaCal35*, 46A06 or 60C09 had been growing prior. Three days later, plates were photographed (C, E, F, G, I and K). White asterisks indicate the spot where *A. niger* spores were inoculated. Photograph A shows growth of *A. niger* by itself on PDA.

induced vascular discoloration, whereas *CaCal35* by itself or *BvFZB42* by itself did not (Fig. 4A). *Colli42* also returned the highest marketable yield of all treatments (i.e. 37.46 US tons of red tomato fruit per acre), but the differences between treatments were not significant (Fig. 4B).

Isolation and characterization of *CaCal35* transposon mutants with reduced antifungal activity

To identify the gene(s) underlying the observed antifungal and biocombicontrol activity of *CaCal35*, approximately 6,500 random EZ-Tn5 transposon insertion mutants of *CaCal35* were generated and screened for reduced antifungal activity against *A. niger* in a bottomless 96-well microtitre plate set-up (see Experimental Procedures). Two such mutants, designated 46A06 and 60C09, were identified (Fig. S2). We confirmed in a standard confrontation assay that both mutants had lost the ability to inhibit hyphal growth of *A. niger* (Fig. 1, panels A3 and A4). Mixing the two mutants together did not result in restoration to wild-type levels of inhibition (Fig. 1, panel A5). Also, *A. niger* appeared unaffected after inoculation onto a PDA plate on which either 46A06 or 60C09 was previously grown (Fig. 2H–I and J–K respectively).

Mutants 46A06 and 60C09 had also lost, completely or partially, the ability to inhibit *Fol*, *Fof*, *R. solani*, *S. rolf-sii*, *S. sclerotiorum* and *V. dahliae* (Fig. 1, B3–G3 and B4–G4 respectively). For none of these fungi did the two mutants achieve wild-type levels of fungal inhibition when mixed together (Fig. 1, B5–F5). *M. grisea* was the

only fungus that was still inhibited by mutant 46A06 as well as 60C09 (Fig. 1, H3 and H4, respectively), suggesting that the transposon insertions in these mutants did not impact *CaCal35*'s suppression of *M. grisea*.

In greenhouse experiments, a mixture of *BvFZB42* and mutant 46A06 did not significantly protect tomato plants from *Fol*-induced loss of biomass, and neither did a mixture of wild-type *CaCal35* and the *BvFZB42* mutant AK3, or a mixture of the two mutants (46A06 and AK3) (Fig. 5A). The reduction in vascular discoloration that was observed with these mixtures was less than that achieved with *Colli42*, but not significantly (Fig. 5B).

Genetic characterization of mutant 46A06

Genomic flank sequencing of the transposon in mutant 46A06 revealed the insertion site as 5'-GTGTACGGA-3' inside locus LT85_RS01670 (Fig. S3A–C). This gene is part of a 76.95-kb region of the *CaCal35* genome (NCBI coordinates 365,248–442,201 of NZ_CP009962.1). This region harbours at least 35 predicted genes (Table 1) and was tagged by antiSMASH as containing a hybrid PKS-NRPS gene cluster. No hybrid PKS-NRPS gene clusters like it were found on the published genomes of other *Collimonas* strains, including *C. fungivorans* Ter6 and Ter331, *C. pratensis* Ter91 and Ter291, *C. arenae* Ter10 and Ter282, and *Collimonas* sp. ES_AI-A1, PA-H2, OK607, OK242, OK412, OK307, and UBA1456. However, we were able to identify gene clusters with similar synteny and predicted function on the genomes of *Chromobacterium violaceum* ATCC 53434 (Parker *et al.*, 1988; Singh *et al.*, 1988), *Chitinimonas koreensis*

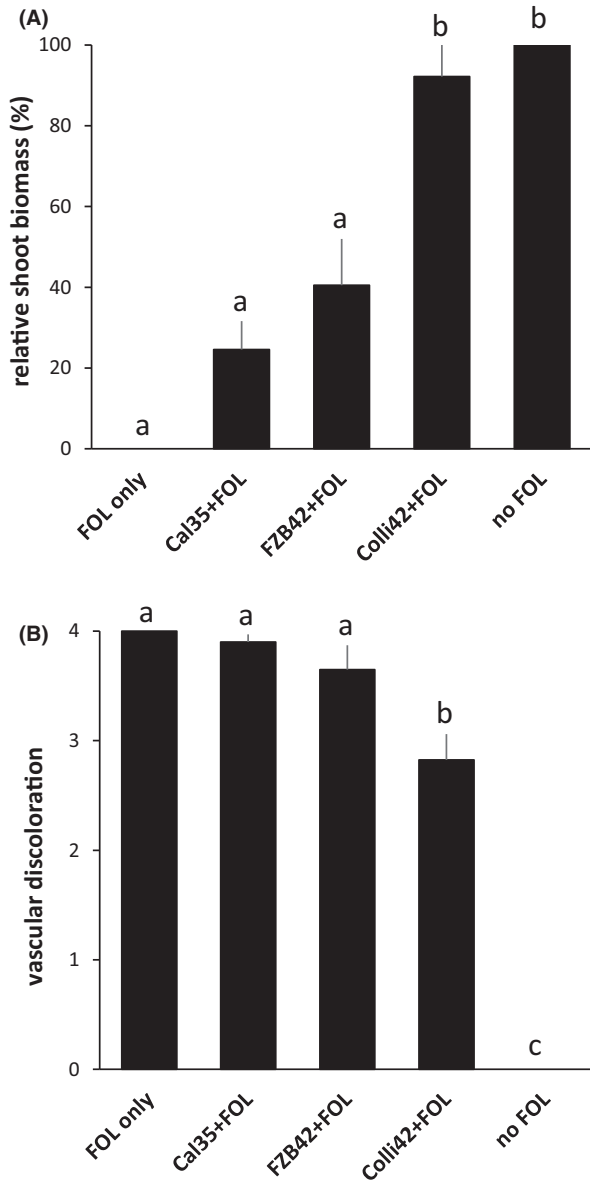


Fig. 3. Ability of *CaCal35* and *BvFZB42*, either by themselves or mixed together (i.e. *Colli42*) to reduce *Fol*-induced symptoms, i.e. loss of shoot biomass (A) or vascular discoloration (B) on tomato plants in greenhouse experiments. Shown are the averages and standard errors from four independent greenhouse experiments. Averages marked with the same letter were not significantly different from each other, as assessed by ANOVA with multiple comparisons using Tukey–Kramer test ($P < 0.05$). Relative shoot biomass (in %) was calculated as explained in the Experimental Procedures section and indicates the degree to which individual bacterial strains or the bacterial mixture were able to rescue tomato plants from harm by *Fol*: boundaries are set by the treatments *Fol*-only and *no-Fol* (0 and 100%, respectively, on the y-axis). Vascular discoloration was assessed on a 0–4 scale, where 0 means no discoloration and 4 means > 40% discoloration.

DSM 17726 (Kim *et al.*, 2006), *Paraburkholderia megapolitana* LMG 23650 (Vandamme *et al.*, 2007) and *Paraburkholderia acidophila* ATCC 31363 (Horsman

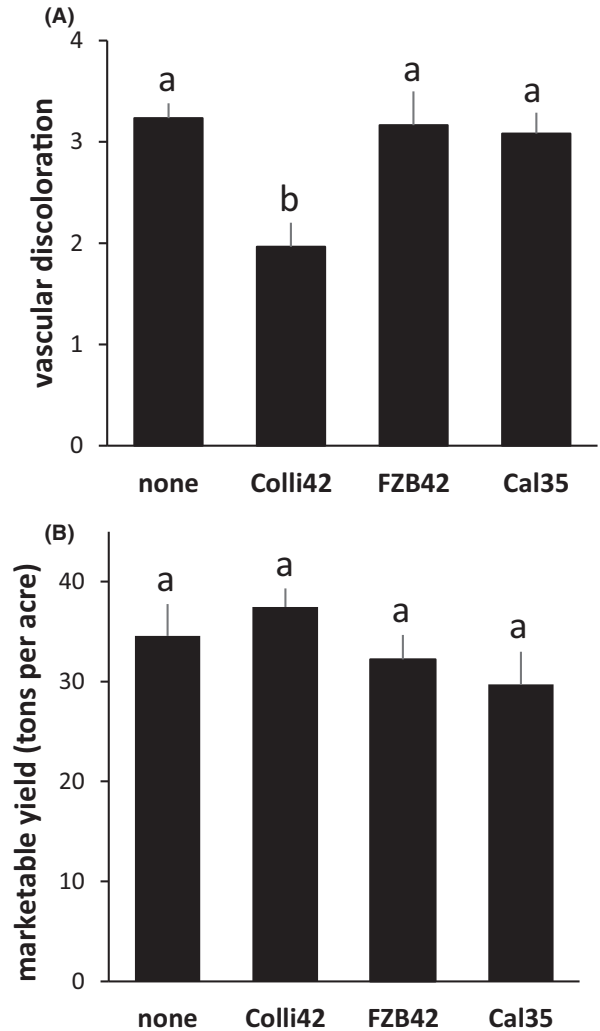


Fig. 4. Ability of *CaCal35* and *BvFZB42*, either by themselves or mixed together (i.e. *Colli42*) to reduce vascular discoloration (A) and yield loss (B) of tomato plants grown in a *Fol*-infested field. For each one of the four treatments (i.e. no bacteria, *Colli42*, *CaCal35* and *BvFZB42*), four plots with 15 plants were set up. Shown are the averages and standard errors for plants across the plots. Bars with the same letter represent averages that were not significantly different from each other, as assessed by ANOVA with multiple comparisons using Tukey–Kramer test ($P < 0.05$).

et al., 2017). The similarity appeared to be limited to a stretch of genes corresponding to LT85_RS01720 → LT85_RS01665 in *CaCal35*, which includes the gene carrying the transposon insertion in 46A06, i.e. LT85_RS01670 (Fig. S4).

LT85_RS01670 is the ninth in a predicted supraoperon of 11 genes (LT85_RS01720 → LT85_RS01660; Fig. 6A, Table S1), which we refer to as *cplABCDEF-GHIJK* (where *cpl* stands for carenaemin production locus). According to the ‘co-linearity rule’ (Fischbach and Walsh, 2006), the first five genes of this supraoperon (*cplABCDE*) were predicted to code for the production of

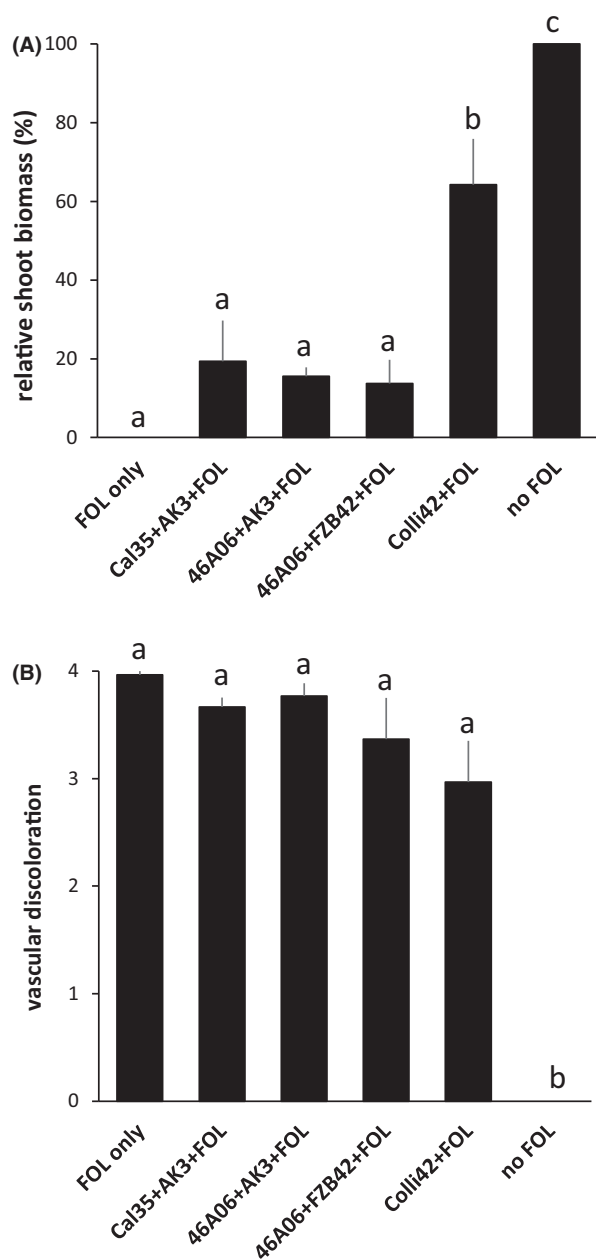


Fig. 5. Comparison of wild-type *CaCal35* to mutant 46A06 in terms of ability to reduce *Fol*-induced symptoms, i.e. loss of shoot biomass (A) or vascular discoloration (B) on tomato plants, in combination with *BvFZB42* or its mutant derivative AK3. Shown are the averages and standard errors from three independent greenhouse experiments. Averages marked with the same letter are not significantly different from each other, as assessed by ANOVA with multiple comparisons using Tukey–Kramer test ($P < 0.05$). Relative shoot biomass (in %) was calculated as explained in the Experimental Procedures section and indicates the degree to treatments were able to rescue tomato plants from harm by *Fol*: boundaries are set by the treatments *Fol*-only and *no-Fol* (0 and 100%, respectively, on the y-axis). Vascular discoloration was assessed on a 0–4 scale, where 0 means no discoloration and four means > 40% discoloration.

a secondary metabolite featuring a core scaffold of three amino acid residues, with the first and second amino acids linked through a peptide bond and the second and third by a $-\text{CH}_2\text{-CHOH}-$ moiety (Fig. 6B and C). The middle amino acid is predicted to be a serine, based both on NRPSPredictor2 and on the Stachelhaus sequence (i.e. DVWHFSLVDK) of the corresponding adenylation domain in the *cplB* gene product. The Stachelhaus sequences of the other two adenylation domains (DIWQFGLILK in *cplA* and DALFMGGVIK in *cplC*) were most similar (but not identical) to those reported for glutamine (DAWQFGLIDK) and leucine (DALVMGAVMK) respectively (Rausch *et al.*, 2005). The presence of an epimerization domain in the predicted *cplC* product suggested that the third amino acid exists in D-configuration in the structure. The presence of a ketosynthase/malonyltransferase domain and an aminotransferase domain at the N-terminal end of the *cplA* gene product puts a predicted $\text{R}_1\text{-CNH}_2\text{-CH}_2\text{-}$ group at one end of the secondary metabolite (which generates a glycine amino acid), with a $-\text{CO-R}_2$ group predicted at the other end, based on the ketosynthase/malonyltransferase domain in *cplD*. The chemical formula of the predicted core structure shown in Fig. 6C, not including R_1 and R_2 , is $\text{C}_{21}\text{H}_{35}\text{O}_8\text{N}_5$, with a predicted mass of 485.53 Da.

The LT85_RS01670 gene (i.e. *cplI*) which carried the transposon insertion in mutant 46A06 is annotated to code for a polysaccharide pyruvyl transferase family protein (accession number WP_081991923). Pyruvyl transferases catalyse the transfer of the pyruvate moiety to a saccharide target (Hager *et al.*, 2019). Proteins belonging to this functional family include *CsaB* (Fujinami and Ito, 2018; Hager *et al.*, 2018), *WcaK* (Stevenson *et al.*, 1996), *AmsJ* (Wang *et al.*, 2012) and *PssM* (Ivashina *et al.*, 2010), which are all involved in the production of exopolysaccharides (EPS), including secondary cell wall polymers in *Bacillus* species, colanic acid in *Escherichia coli*, amylovoran in *Erwinia* and EPS in *Rhizobium leguminosarum* respectively. Immediately downstream of *cplI* and part of the same predicted operon as *cplI* are *cplJ* (LT85_RS01665) and *cplK* (LT85_RS01660), annotated as a hypothetical protein and a deaminated glutathione amidase respectively.

Genetic characterization of 60C09. In mutant 60C09, the EZ-Tn5 transposon was found inserted into the sequence 5'-GTATAAGCA-3', where TAA is the stop codon for gene LT85_RS04520 (Fig. S3D–F). Multiple genes in the immediate vicinity of LT85_RS04520 (Fig. 6B; Table 2) are predicted to contribute to the so-called Wzy-dependent pathway for synthesis and incorporation of oligosaccharide repeat units into cell

Table 1. Genomic context of the transposon insertion in CaCal35 mutant 46A06.^a

NCBI locus tag	Predicted protein	NCBI protein ID
LT85_RS01600	Acetyl-CoA C-acyltransferase	WP_038484473.1
LT85_RS01615	SDR family oxidoreductase	WP_038484482.1
LT85_RS01625	Hypothetical protein	WP_038484490.1
LT85_RS01630	DGQHR domain-containing protein	WP_156117397.1
LT85_RS01635	LysE family translocator	WP_038484493.1
LT85_RS01640	Lrp/AsnC family transcriptional regulator	WP_038484496.1
LT85_RS01645	VOC family protein	WP_038484499.1
LT85_RS01650	MarR family transcriptional regulator	WP_038484502.1
LT85_RS01655	TCR/Tet family MFS transporter	WP_052135471.1
LT85_RS01660	Deaminated glutathione amidase	WP_172656931.1
LT85_RS01665	Hypothetical protein	WP_156117398.1
LT85_RS01670	Polysaccharide pyruvyl transferase family protein	WP_038484508.1
LT85_RS01675	4'-phosphopantetheinyl transferase superfamily protein	WP_052134537.1
LT85_RS01680	Thioesterase	WP_052134540.1
LT85_RS01685	Polyunsaturated fatty acid/polyketide biosynthesis protein	WP_052134542.1
LT85_RS01690	Hypothetical protein	WP_038484511.1
LT85_RS01695	Type I polyketide synthase	WP_038484514.1
LT85_RS01700	Non-ribosomal peptide synthetase	WP_052134544.1
LT85_RS01715	Hybrid non-ribosomal peptide synthetase/type I polyketide synthase	WP_081991927.1
LT85_RS01720	Hybrid non-ribosomal peptide synthetase/type I polyketide synthase	WP_038484528.1
LT85_RS01725	Helix-turn-helix transcriptional regulator	WP_038484531.1
LT85_RS01730	SDR family oxidoreductase	WP_081991930.1
LT85_RS01735	LysR family transcriptional regulator	WP_052134547.1
LT85_RS01740	alpha/beta hydrolase	WP_038484534.1
LT85_RS25150	Pirin family protein	WP_009049067.1
LT85_RS01750	NmrA/HSCARG family protein	WP_017604182.1
LT85_RS01755	Phosphoesterase	WP_052134552.1
LT85_RS01760	c-type cytochrome	WP_052135472.1
LT85_RS01765	Branched-chain amino acid transferase	WP_038484543.1
LT85_RS01775	NAD(P)-dependent alcohol dehydrogenase	WP_038484549.1
LT85_RS01780	AraC family transcriptional regulator	WP_038494762.1
LT85_RS01785	LysR family transcriptional regulator	WP_038484552.1
LT85_RS01790	SDR family oxidoreductase	WP_038484555.1
LT85_RS01795	SnoaL-like domain-containing protein	WP_038484558.1
LT85_RS01800	DEAD/DEAH box helicase	WP_081991932.1

a. Highlighted in bold is the gene (LT85_RS01670) that carried the transposon insertion in 46A06. This gene is part of the *cplABCDEFGHIJK* supraoperon (where *cpl* stands for carenaemin production locus, LT85_RS01720 → LT85_RS01660) which is highlighted in grey.

surface lipopolysaccharides (Kalynych *et al.*, 2014). This pathway involves the initial transfer of a sugar moiety to a lipid carrier (probably catalysed by the product of LT85_RS04530), the addition of sugar groups by glycosyltransferases (LT85_RS25805, LT85_RS04525) to generate an oligosaccharide repeat unit. Individual units are transported into the periplasm by a Wzx flippase (LT85_RS04500), where they undergo polymerization by a Wzy polymerase (LT85_RS25800) to yield a polysaccharide that then may be transferred to the inner-core oligosaccharide of lipid A by WaaL ligase (LT85_RS04650) and transported to the cell surface.

One of the sugars in the oligosaccharide repeat unit probably is rhamnose, seeing that (i) LT85_04485, _04480, _04490 and _04495 resemble the *rmlABCD* genes for the conversion of D-glucose-1-P into deoxythymidine diphosphate (dTDP)-L-rhamnose (King *et al.*, 2009), and (ii) the LT85_RS25805 gene product is highly similar to RfbF, which is a dTDP-rhamnosyl transferase that in *Shigella flexneri* generates the N-

acetylglucosamine-Rha-Rha-Rha tetrasaccharide repeat (Morona *et al.*, 1995). Another sugar in the oligosaccharide repeat unit may be 6-deoxytalose, given that the two genes flanking LT85_RS04520 are predicted to code for the conversion of dTDP-L-rhamnose into dTDP-L-6-deoxytalose (LT85_04515) and for adding dTDP-L-6-deoxytalose to the growing oligosaccharide repeat unit (LT85_04525), based on similarity to the *tle* and *gtr29* gene products, respectively, from *Acinetobacter baumannii* (Kenyon *et al.*, 2017). The LT85_RS04520 product itself is annotated as a serine acetyltransferase. It showed substantial homology to WcaB from *E. coli* which also carries the signature of a serine acetyltransferase, but has been shown to catalyse the acetylation of a galactosyl residue after its incorporation as the fourth sugar into the heptasaccharide repeat unit of colanic acid (Scott *et al.*, 2019). This acetylation enables the next glycosyltransferase to add the fifth sugar onto the colanic acid repeating unit (Scott *et al.*, 2019).

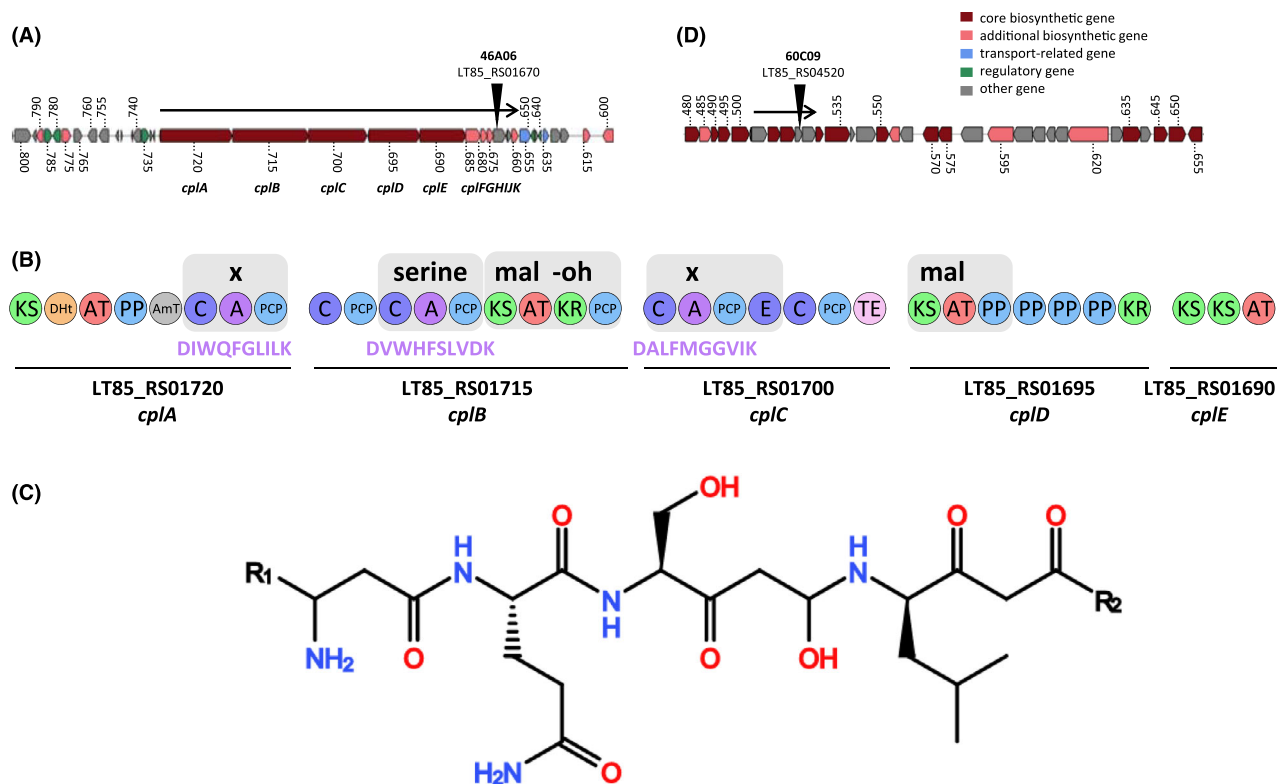


Fig. 6. Schematic representation of the two loci on the chromosome of *CaCal35* involved in carenaemin synthesis and identified in mutants 46A06 (A) and 60C09 (B), respectively, along with an AntiSMASH-based analysis of the *cplABCDE* genes (C) and the predicted structure of the *cplABCDE*-encoded product. In panels A and B, genes are coloured according to predicted functions as indicated by the legend. Black triangle heads indicate the transposon insertion sites in gene LT85_RS01670 in mutant 46A06 (A) or gene LT85_RS04520 in mutant 60C09 (B). Individual genes are labelled with their NCBI gene locus tag. Arrows represent predicted operons as determined by FgenesB (<http://www.softberry.com>). Panel B shows the PKS and NRPS domain architectures as predicted by antiSMASH: A: adenylation, C: condensation, PCP: peptidyl carrier protein, ACP: acyl carrier protein, E: epimerase, TE: thioesterase, KS: beta-ketoacyl synthase, AT: acyltransferase, KR: beta-ketoacyl reductase and DHT: dehydratase domain. The Stachelhaus sequences for each of the three adenylation domains (one in *cplA*, one in *cplB* and one in *cplC*) are shown in purple lettering.

Characterization of the antifungal activity produced by *CaCal35*

We were unsuccessful in our efforts to recover antifungal activity from culture supernatants of *CaCal35* grown in broth. We therefore devised an agar diffusion assay to extract antifungal activity from *CaCal35* grown on agar instead. This assay (Fig. S5) exploits the fact that such activity is produced by *CaCal35* on agar in the absence of fungus and is diffusible through agar. The diffusates that were collected in this way from wild-type *CaCal35* and from mutants 46A06 and 60C09 were tested in a modified confrontation assay with *A. niger* to reveal that hyphal growth of *A. niger* was reduced in the presence of diffusates extracted from *CaCal35*, but not with those extracted from mutants 46A06 and 60C09 (Fig. 7A). The diffusates were analysed by liquid chromatography–mass spectrometry, revealing two prominent peaks (labelled as a and b in Fig. 7B) that were present in the *CaCal35*

diffusate but absent in the diffusates collected from the mutants 46A06 (Fig. 7C) and 60C09 (Fig. 7D). These two peaks eluted with retention times of 13.3 and 13.7 min, and *m/z* values of 835.493 and 849.509 Da, respectively, in both negative and positive mode. The difference in *m/z* between peaks a and b equals 14.016 Da, which approximates (Patiny and Borel, 2013) the mass of a CH₂ moiety. Furthermore, we observed two peaks that were unique to the diffusate from mutant 46A06 and absent from those of wild-type *CaCal35* and mutant 60C09 (labelled as c and d in Fig. 7C). These peaks had retention times of 12.3 and 12.8 min, and *m/z* values were 765.488 and 779.503 Da in both negative and positive mode respectively. The difference in *m/z* between peaks c and d was 14.015, i.e. the same difference in *m/z* as between peaks a and b, and consistent with a CH₂ moiety. In positive mode, the differences in *m/z* between peaks a and c and between peaks b and d were 70.006 and 70.005, respectively, which corresponds with a C₃H₂O₂ moiety.

Table 2. Genomic context of the transposon insertion in CaCal35 mutant 60C09.^a

NCBI locus tag	Predicted protein	NCBI protein ID
LT85_RS04480	dTDP-glucose 4,6-dehydratase (RmlB)	WP_038485799.1
LT85_RS04485	Glucose-1-phosphate thymidyltransferase (RmlA)	WP_038485802.1
LT85_RS04490	dTDP-4-dehydrorhamnose 3,5-epimerase (RmlC)	WP_038485806.1
LT85_RS04495	dTDP-4-dehydrorhamnose reductase (RmlD)	WP_038485809.1
LT85_RS04500	flippase	WP_081992030.1
LT85_RS25800	Oligosaccharide repeat unit polymerase	WP_081992033.1
LT85_RS25805	dTDP-L-rhamnosyltransferase	WP_081992035.1
LT85_RS04515	dtdp-L-rhamnose 4 epimerase (Tie)	WP_038495031.1
LT85_RS04520	Serine acetyltransferase	WP_038485818.1
LT85_RS04525	dTDP-6-deoxy-L-talosyltransferase	WP_038485820.1
LT85_RS04530	Lipid carrier: UDP-N-acetylgalactosaminyltransferase	WP_038485823.1
LT85_RS04535	UDP-N-acetylglucosamine 4,6-dehydratase	WP_052134643.1
LT85_RS04540	H-NS histone family protein	WP_038485826.1
LT85_RS04545	Phosphomannomutase/phosphoglucomutase	WP_038485829.1
LT85_RS04550	Lipopolysaccharide heptosyltransferase I	WP_038485833.1
LT85_RS25195	Class I SAM-dependent methyltransferase	WP_081992037.1
LT85_RS04560	Hypothetical protein	WP_038485836.1
LT85_RS04565	Class I SAM-dependent methyltransferase	WP_172656939.1
LT85_RS04570	Glycosyltransferase	WP_052134650.1
LT85_RS04575	Glycosyltransferase	WP_038485842.1
LT85_RS04580	Hypothetical protein	WP_038485845.1
LT85_RS04585	DUF2142 domain-containing protein	WP_172656940.1
LT85_RS04595	Selenocysteine-specific translation elongation factor	WP_038485851.1
LT85_RS04600	L-seryl-tRNA(Sec) selenium transferase	WP_052134652.1
LT85_RS04605	Formate dehydrogenase accessory protein FdhE	WP_038485854.1
LT85_RS04610	Formate dehydrogenase subunit gamma	WP_038485857.1
LT85_RS04615	Formate dehydrogenase subunit beta	WP_038485861.1
LT85_RS04620	Formate dehydrogenase-N subunit alpha	WP_156117426.1
LT85_RS04625	Sulfate ABC transporter substrate-binding protein	WP_038485868.1
LT85_RS04630	3-deoxy-D-manno-oct-2-ulonic acid (Kdo) hydroxylase	WP_038485871.1
LT85_RS04635	3-deoxy-D-manno-octulosonic acid transferase	WP_038495045.1
LT85_RS04640	YdcF family protein	WP_038485874.1
LT85_RS04645	Glycosyl transferase	WP_052134654.1
LT85_RS04650	O-antigen ligase domain-containing protein	WP_038485877.1
LT85_RS04655	UDP-glucose 4-epimerase GalE subunit	WP_038485880.1

a. Highlighted in bold is the gene (LT85_RS04520) that carried the transposon insertion in 60C09. This gene is part of a predicted operon (highlighted in grey).

Discussion

Our data revealed that the ability of CaCal35 to inhibit the growth of a wide range of fungal species, including *A. niger* and *Fusarium oxysporum* f.sp. *lycopersici* (Fo), depends on the production and secretion of an antimycotal activity that we call carenaemin. We showed that this activity is water-soluble, diffusible, and produced in the absence of fungus. The activity was lost in two transposon insertion mutants (46A06 and 60C09) which led us to two gene loci of interest, on different parts of the CaCal35 chromosome.

Characterization of mutant 46A06 identified the *cpl* cluster as a major contender for involvement in the synthesis of carenaemin by CaCal35. This cluster codes for a hybrid PKS/NRPS that is predicted to produce a metabolite that has the amino acids Gln, Ser and Leu at its core (Fig. 6). Interestingly, the observation that the diffusate of wild-type Cal35 showed two major peaks (a and b) that differed in mass by a CH₂ group may be

explained by assuming promiscuity for one of the adenylation domains in the *cpl* gene cluster. Such promiscuity, more specifically as it relates to accepting two amino acids that differ by one CH₂ group in their side-chain, is not uncommon (Qiao *et al.*, 2011). For all three predicted amino acids in the carenaemin core (Gln, Ser, and Leu), there exists a corresponding amino acid that differs by only one CH₂ group (Asn, Thr and Val, respectively), so it is unclear which one of the three adenylation domains in the *cpl* gene cluster might be the promiscuous one. The same difference of one CH₂ group was also observed between the two major peaks in the diffusate of the 46A06 mutant (peaks c and d). This suggests that the metabolites produced by this mutant, while lacking antifungal activity, likely contain the same peptide core as the active metabolites produced by wild-type Cal35. This is also consistent with the observation that the transposon insertion in 46A06 was not located inside of the *cplABCDE* genes that are presumed to be involved in the synthesis of the core.

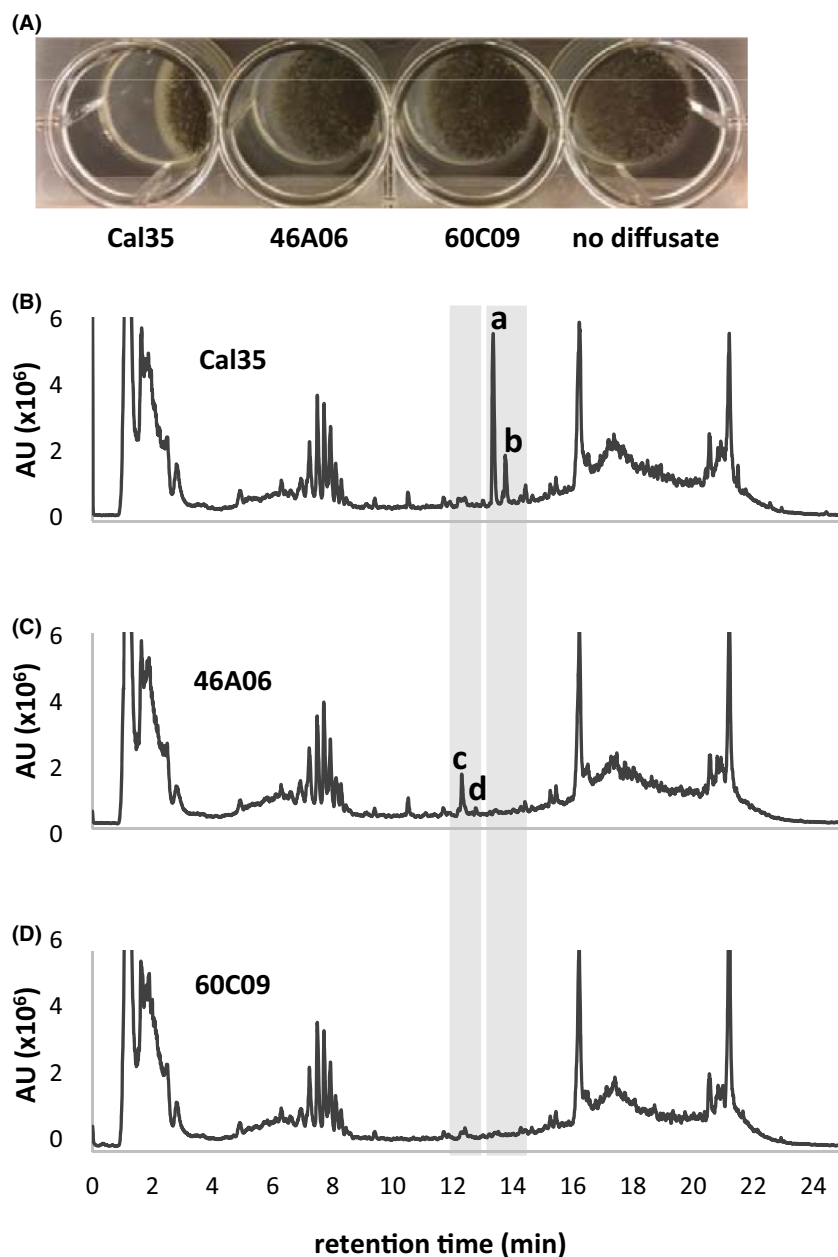


Fig. 7. Antifungal activity (or lack thereof) in diffusates from wild-type *CaCal35* and mutants 46A06 and 60C09 (A) and LC-MS chromatograms of these same diffusates (B–D). In panel B, a and b represent two peaks that were present in diffusate from *CaCal35*, but absent in mutants 46A06 and 60C09. In panel C, c and d represent two peaks that were present in diffusate from 46A06, but absent from *CaCal35* and 60C09. See text for more details on these peaks.

Instead, the transposon in mutant 46A06 was found inserted into a gene that lies downstream of *cplABCDE* and is predicted to code for a polysaccharide pyruvyl transferase. This annotation suggests a link between the production of the carenaemin peptide core and the polysaccharide synthesis gene cluster that was identified through mutant 60C09. Pyruvyl transferases add a pyruvyl group to monosaccharides and are typically mentioned in the context of cell surface polysaccharides

(Hager *et al.*, 2019). One typical outcome of pyruvyl transferase activity is the formation of a ketal structure which bridges two hydroxyl groups of a monosaccharide residue through pyruvate, thus forming a ring structure (Hager *et al.*, 2019). In this process, two hydrogens (2H) are removed from the sugar moiety and a $C_3H_4O_2$ group is added back, for a net addition of $C_3H_2O_2$, which represents a monoisotopic mass of 70.005. Interestingly, this mass equals the difference that we found in positive and

negative mode between the m/z values of peaks a and c and between the m/z values of peaks b and d in the diffusates of wild type and 46A06 respectively. Seeing that the diffusate of 46A06 lacked antifungal activity altogether, the simplest explanation for the difference in m/z between peaks a/b and c/d is that pyruvylation is required for antifungal activity. Because pyruvyl transferases act on monosaccharides, this conclusion also implies that carenaemin features at least one sugar moiety.

As for the nature of the purported sugar moiety in carenaemin, rhamnose and 6-deoxytalose are obvious candidates, given the proximity of the transposon insertion in mutant 60C09 to genes involved in the biosynthesis of dTDP-L-rhamnose and dTDP-L-6-deoxytalose. Metabolites that have antibiological activity and feature rhamnose as a decoration include caprazamycin (Kaysner *et al.*, 2010), spinosyn A (Chen *et al.*, 2009), elloramycin (Blanco *et al.*, 2001) and brabantamide (Schmidt *et al.*, 2014), as well as the antifungals thailandin A (Greule *et al.*, 2016) and hassallidin B (Neuhof *et al.*, 2006). Also, rhamnose, together with 6-deoxytalose, is a key component of the so-called non-specific glycopeptidolipids (GPLs) in the outer layer of the cell wall of non-tuberculosis mycobacteria (Mullowney *et al.*, 2018). It is known that rhamnose can be pyruvylated (Pan *et al.*, 2015), and the differences between the m/z values of peaks a, b, c and d in the *CaCal35* and 46A06 diffusates (835.5, 849.5, 765.5 and 779.5, respectively) and the calculated molecular mass of the predicted peptide core (485.5 Da) are sufficiently large (350 and 364 Da for *CaCal35*; 280 and 294 Da for 46A06, respectively) to be consistent with the presence of one pyruvylated rhamnosyl group (233.1 Da) or one non-pyruvylated rhamnosyl group (163.1 Da).

Worthwhile to note is that the transposon insertion in *CaCal35* mutant 60C09 was not actually inside one of the sugar biosynthetic genes. This excludes the possibility that the failure to synthesize these sugars underlies the inability of mutant 60C09 to produce carenaemin. Also, we did not see in the diffusate of mutant 60C09 a unique compound (i.e. not found in the diffusates of *CaCal35* or mutant 46A06) which could be interpreted as an aglyconic version of carenaemin. In other words, mutant 60C09 would appear to have the potential to produce the carenaemin core (it has an intact *cpI* gene cluster after all) and to synthesize the sugar(s) presumably needed to decorate the core, but its diffusate shows neither a sugar-bearing nor a sugar-free core. This observation is consistent with a scenario in which (i) the gene cluster knocked out in mutant 60C09 is responsible for attaching the sugar to the core and (ii) attachment of the sugar is necessary for secretion of the sugar-bearing core (seeing that secretion is a requirement for being

detectable in the diffusate). Considering that we were able to detect what is assumed to be a sugar-decorated but non-pyruvylated core in the diffusate of mutant 46A06, pyruvylation seems to be unimportant for adding sugar to the core or for secretion of the sugar-bearing core.

The prediction that the gene cluster knocked out in 60C09 codes for the Wzy-dependent synthesis and export of oligosaccharide repeat units offers a possible mechanism for the observed coupling of glycosylation and secretion of carenaemin. The mechanism we propose here resembles steps involved in the synthesis and export of peptidoglycan units, where in the cytoplasm a pentapeptide is attached to a Lipid-II-bound disaccharide (*N*-acetylglucosamine-*N*-acetylmuramic acid) which then is transported across the membrane (Breukink and de Kruijff, 2006; de Kruijff *et al.*, 2008). Similarly, the 46A06-produced peptide core may be attached to one of the sugars in the repeat unit of rhamnose and/or 6-deoxytalose that then gets flipped into the periplasm. Additional studies will be needed to test this hypothesis, to identify the enzyme responsible for attaching the 46A06-produced peptide core to the sugar repeat (pyruvylated or not) and to elucidate the steps that lead from the transport into the periplasm to the secretion of carenaemin.

An alternative scenario that is consistent with our observations is that the substrate that is loaded onto the KS domain encoded by *cpI*A needs to be glycosylated before it can be accepted as a substrate for subsequent *cpI*ABCDE-encoded reactions leading to carenaemin. A similar scenario has been proposed for brabantamide, where the inability to detect an aglyconic (i.e. non-rhamnosylated) version of brabantamide was explained by assuming that the glycosylation reaction occurs early in the biosynthesis, not as a late-stage tailoring step (Schmidt *et al.*, 2014). This alternative hypothesis for the synthesis and secretion of carenaemin will also require further experimental scrutiny, in order to identify the protein(s) responsible for the extracellular delivery of carenaemin and to explain the involvement of components of the Wzy-dependent pathway that are knocked out in 60C09.

Both of the scenarios described above are consistent with our observation that mutants 46A06 and 60C09 were unable to complement each other and restore antifungal activity to wild-type *CaCal35* levels. In the first scenario, mutant 60C09 would be unable to secrete the peptide core and to make it available to 46A06 for glycosylation. In the second scenario, the 46A06-produced glycosylated substrate for CplABCDE would need to be secreted and taken up by 60C09 for production of functional carenaemin, which is unlikely.

The absence of a carenaemin biosynthesis gene cluster from other known *Collimonas* genomes suggests that

CaCal35 acquired the *cpl* genes horizontally from unrelated bacteria. We can assume that the *cpl* genes confer upon *CaCal35*, and upon the alleged donor, an advantage over other bacteria with which they shared the same environment. Collimonads are typically found in nutrient-poor conditions (Leveau *et al.*, 2010) and a bacterium like *CaCal35*, which was isolated from the mineral horizon of a forest soil (Uroz *et al.*, 2014) may benefit from carenaemin as a means to suppress fungal growth and exploitation of shared but limited resources. Of interest in this context is the reported origin of *Paraburkholderia megapolitana* LMG 23650, which is one of the strains we identified as carrying a *cpl*-like gene cluster in its genome (see Results section). This strain was originally isolated as *Burkholderia phenazinium* A3 from moss plants on the southern coast of the Baltic Sea in Germany (Vandamme *et al.*, 2007). The site where A3 was found has been described as a nutrient-poor habitat, and A3 has been shown to possess antifungal activity (Opelt and Berg, 2004). Interestingly, from the same habitat, as part of the same expedition that unearthed A3, a *Collimonas fungivorans* isolate was recovered, labelled A23 (Opelt and Berg, 2004). This strain too was shown to have antifungal activity, specifically against *V. dahliae* (Opelt and Berg, 2004), *Botrytis cinerea* (Sylla *et al.*, 2012), and *Phytophthora cactorum* and *P. fragariae* (Bisutti and Stephan, 2011). However, it remains unknown whether the A23 genome harbours a *cpl* gene cluster, and whether this gene cluster underlies the antifungal activities of A23 and A3 and contributes to their fitness in the nutrient-poor phytobiomes from which they were isolated.

In greenhouse and field experiments, *CaCal35* suppressed the formation of symptoms by soilborne pathogen *Fol* on tomato plants, but only in combination with *BvFZB42* (i.e. as a *Colli42* mixture). Neither *CaCal35* by itself, nor *BvFZB42* by itself, had the ability to protect tomato plants. The same result was recently reported for a mixture of *CaCal35* and the commercially available biofungicide Serenade Soil (active ingredient: *BvQST713*) (Doan *et al.*, 2020). This emerging protective property of *Collimonas-Bacillus* mixtures has been dubbed 'biocombicontrol' (Doan *et al.*, 2020). Seeing that mutant 46A06 did not show synergy with *BvFZB42* under greenhouse conditions suggests that carenaemin contributes to the biocombicontrol phenomenon of *Colli42*. Similarly, the AK3 mutant of *BvFZB42*, unable to produce bacillomycin D and fengycin (Koumoutsi *et al.*, 2004), did not show synergy with *CaCal35* in our experiments. These observations lead us to hypothesize that the observed synergy between *Collimonas* and *Bacillus* is a result of the synergy between the antifungal metabolites that these bacteria produce. This hypothesis is practically relevant: seeing that Serenade Soil is one of

the most popular *Bacillus*-based biofungicidal products on the market and that *BvFZB42* is the active ingredient of the commercially available biocontrol product RhizoVital® 42 liquid (Borriss, 2011) and is a closely related 'cousin' of FZB24, which is the active ingredient in the commercially available formulation Taegro (Fan *et al.*, 2018), the question can be asked whether all these and other *Bacillus*-based products might work even better by amending them with *CaCal35*.

Experimental procedures

Microbial strains and growth conditions

All bacterial strains used in this study were stored as glycerol stocks at -80°C , and grown in King's medium B (KB; 20 g Bacto Proteose Peptone No.3, 1.15 g K_2HPO_4 , 0.73 g $\text{MgSO}_4 \cdot 7\text{H}_2\text{O}$, 10 ml glycerol per litre) or on KB agar (KB supplemented with 16 g agar per litre) or Potato Dextrose Agar (PDA) (39 g Difco Potato dextrose agar per litre). *CaCal35* was originally isolated from forest soils (Uroz *et al.*, 2014; Wu *et al.*, 2015). *BvFZB42* and its mutant AK3 were obtained from the Bacillus Genetic Stock Center (BGSC, Columbus, OH, USA). *Aspergillus niger* N402 (ATCC 64974; a derivative of CBS120.49, densely sporulating with short conidiospores) (Bos *et al.*, 1988) has been used previously in confrontation assays with collimonads (Mela *et al.*, 2011; Fritsche *et al.*, 2014; Doan *et al.*, 2020; Mosquera *et al.*, 2020). *Fusarium oxysporum* f.sp. *lycopersici* (*Fol*) race 3 strain D12 (Doan *et al.*, 2020), *F. oxysporum* f.sp. *fragariae* (*Fof*) strain GL1080, *Magnaporthe grisea* strain GL787, *Rhizoctonia solani*, *Sclerotium rolfsii*, *Sclerotinia sclerotiorum* and *Verticillium dahliae* strain T9 were gifted by Dr. Mike Davis (University of California, Davis, CA, USA). All fungal cultures were maintained as spore suspensions in glycerol stocks at -80°C or as mycelium on PDA.

Confrontation assays

Collimonas bacteria were streaked from -80°C glycerol stocks onto KB agar plates and incubated at 28°C for 3 days. To prepare fungal spore suspensions, two- to three-week-old PDA cultures (9 cm diameter petri dish) of *A. niger*, *Fol* or *V. dahliae* were flooded with 15 ml autoclaved water. Spores were suspended using a sterile glass slide and filtered through four layers of sterile cheese cloth (Doan and Davis, 2014). Spore concentrations were determined with a Neubauer Levy Ultra Plane Hemocytometer (Hausser Scientific, Horsham, PA, USA) and adjusted to 10^5 spores per ml with autoclaved water. For *S. rolfsii*, single mature sclerotia obtained from two- to three-week-old cultured PDA plates were used as a source of inoculum. For *Fof*, *R. solani*, *S. sclerotiorum*

and *M. grisea*, we used agar plugs excised from two-week-old PDA cultures.

Confrontation assays were performed as described (Fritsche *et al.*, 2014) except that PDA was used instead of *N*-acetylglucosamine-supplemented water yeast agar. In a petri dish (9 cm diameter) containing 30 ml PDA, *Collimonas* bacteria were line-inoculated on one half of the plate. Five microlitres of a suspension of 10^5 fungal spores per ml in water (*A. niger*, *Fol* or *V. dahliae*), single matured sclerotia (*S. rolfsii*) or agar plugs (*Fof*, *R. solani*, *S. sclerotiorum* and *M. grisea*) was inoculated on the other half of the plate, approximately 2 cm from the bacterial line. Control plates were inoculated with fungi only, i.e. no bacteria. The plates were sealed with parafilm and incubated at 28°C.

To test the diffusibility of the *Collimonas* antifungal activity, bacteria were line-inoculated as before in petri dishes containing 30 ml of PDA per plate. The plates were incubated at 28°C for 3 days, after which the section of agar covered with the bacteria was cut out and removed using a sterile surgical blade. Five microlitres of a suspension of 10^5 *A. niger* spores per ml in water was then spot-inoculated on the remaining section of agar at increasing distances (approximately 1.5, 3 or 4.5 cm) from where the original bacterial line was. The plates were incubated for 3 days at 28°C, assessed for growth by *A. niger* and photographed.

Transposon mutagenesis of *CaCal35*

In a 500 ml flask, 100 ml of KB was inoculated with 1 ml of an overnight pre-culture of *CaCal35* and incubated at 28°C with shaking until the optical density at 600 nm (OD_{600}) reached 0.5–0.7 (~6 h). Two 45 ml culture aliquots were transferred to 50 ml centrifuge tubes (Fisher Scientific, Pittsburgh, PA, USA) and incubated on ice for 30 min. The cells were then harvested by centrifugation at 2500 *g* for 15 min at 4°C. Supernatants were removed, and cells were resuspended in 2 x 25 ml of ice-cold Milli-Q water and centrifuged as before. After discarding the supernatant, cells were resuspended in 2 x 5 ml of ice-cold 10% glycerol in Milli-Q water. After another round of centrifugation, the cells were resuspended in 1 ml of ice-cold 10% glycerol. Fifty μ l aliquots of this suspension were dispensed in microcentrifuge tubes and stored at –80°C for future use, or mixed with no more than 1 μ l of EZ-Tn5 transposome (Epicentre, Madison, WI, USA). After a few minutes on ice, the mixture was transferred to a sterile 0.1 cm electroporation cuvette (Bio-Rad, Hercules, CA, USA) and incubated on ice for 2–3 min. Electroporation was performed with a Bio-Rad Gene Pulser apparatus with the following settings: 25 μ F, 200 ohms and 1.8 kV. Immediately after electroporation, 1 ml of SOC medium (Sambrook and

Russel, 2001) was added to the cuvette and gently mixed by pipetting. The suspension was transferred to a 17 x 100 mm polypropylene tube (Fischer Scientific, Santa Clara, CA, USA) and incubated for 1 h at 28°C with gentle shaking. Part of the suspension was stored as a glycerol stock at –80°C for future plating. Another part was immediately diluted and spread on KB agar plates with 50 μ g of kanamycin per ml and incubated up to three days at 28°C for the selection of transposon insertion mutants. Mutant colonies were restreaked onto fresh KB agar supplemented with 50 mg kanamycin per litre with 48 mutants per plate and incubated for 3 days at 28°C. In total, 6,500 mutants were prepared in this way and screened for loss of antifungal activity, as described below.

Screening for *CaCal35* mutants with reduced antifungal activity

Following the method described previously (Fritsche *et al.*, 2014), the *CaCal35* transposon library was screened for mutants with reduced or abolished antifungal activity towards *A. niger* in bottomless 96-well microtitre plates (Greiner Bio-One, Monroe, NC, USA). For this, the underside of the plates was sealed temporarily with sealing mats (Greiner Bio-One, Frickenhausen, Germany) and each well was filled with molten 250 μ l PDA which was allowed to solidify. Afterwards, the sealing mat was removed and the agar in each well was inoculated on the bottom with one of the 6,500 *Collimonas* mutants (see above), while the top was inoculated with 3 μ l of a 10^5 ml⁻¹ spore suspension of *A. niger*. The plates were incubated at 28°C for 2 days and observed daily for hyphal growth of *A. niger*. Among the 6500 mutants screened, two mutants (46A06 and 60C09) showed reduced antifungal activity, which was confirmed by retesting the two mutants in a standard confrontation assay on PDA (described above).

Identification of transposon insertion sites in *CaCal35* mutants 46A06 and 60C09

The transposon insertion site for mutants 46A06 and 60C09 was determined by genomic flank sequencing as described elsewhere (Tecon and Leveau, 2016). For this, genomic DNA was isolated from 2 ml of an overnight culture of each mutant using the DNeasy blood and tissue kit (Qiagen, Germantown, MA, USA) and resuspended in 50 μ l of elution buffer. Three μ l of DNA (~300–600 ng) in a total volume of 10 μ l was further digested with 10 U of *Eco*RI or *Sac*I (neither one of which cuts in the transposon) for 1 h at 37°C, followed by thermal inactivation at 65°C for 20 min. One μ l of digested DNA was self-ligated in a final volume of 10 μ l

with 1000 U of T4 DNA ligase, for 2 h at room temperature. Two μl of ligation mixture was used as target DNA in a 25 μl PCR using primers KAN-2 FP1 (5'-ACCTA-CAACAAAGCTCTCATCAACC-3') and KAN-2 RP1 (5'-GCAATGTAACATCAGAGATTTTGAG-3') at a concentration of 500 nM each. The reaction cycle was as follows: 95°C for 4 min; 30x [95°C for 30 sec, 55°C for 30 sec, 72°C for 90 sec]; 72°C for 5 min. Amplicons were separated and visualized on a 0.8% agarose gel, and purified from the gel using a QIAquick kit (Qiagen). PCR products were sequenced using primers KAN-2 FP1 and KAN-2 RP1. The flanking DNA sequences were mapped onto the genome sequence (NCBI accession number NZ_CP009962.1) of *C. arenae* Cal35 (Wu *et al.*, 2015). The predicted function of the identified genes and gene clusters and the organization of genes into putative operons were assessed using the NCBI database, the biosynthetic gene cluster identification tool antiSMASH version 5.0.0 (<https://www.antismash.com>) (Medema *et al.*, 2011) and the FGENESB online software at <http://www.softberry.com> (Solovyev and Salamov, 2011). Efforts to complement mutants 46A06 and 60C09 with full-length copies of the genes that carried a transposon insertion on their chromosomes were not successful.

Collection and characterization of CaCal35, 46A06 and 60C09 diffusates

In order to extract antifungal activity from PDA-grown wild type and mutant CaCal 35 strains, we used a sterile, 10 mm diameter cork borer to generate 10 wells in the agar of five PDA plates per strain. These wells were separated by about 2 mm and arranged in a U-shaped pattern (Fig. S5). CaCal35 or its mutant derivatives 46A06 and 60C09 were inoculated onto these PDA plates, with a distance of approximately 1 cm from the edge of the wells. The plates were sealed with parafilm and incubated at 28°C. Three days later, each well was filled with up to 250 μl of PDB (i.e. Potato Dextrose Broth), after which the plates were sealed again with parafilm and incubated at room temperature (23°C) in the dark. After 3, 6, 24 and/or 48 h, aliquots were taken from the PDB in the wells and pooled for each plate. These pooled aliquots, referred to as diffusates, were filtered (0.2- μm) and tested in a modified confrontation assay against *A. niger*, as follows. Each well of a 12-well microtitre plate was filled with 1 ml molten PDA, and after it had solidified, 3 microlitres of an *A. niger* spore suspension (10^5 spores/ml in water) was inoculated onto the agar surface at one end of each well, as were 50 μl of CaCal35, 49A06 or 60C09 diffusate at the opposite end of the same well. As a control for the diffusate, we pipetted 50 μl of sterile PDB. Plates were sealed with

parafilm and incubated at 28°C. The plates were observed and photographed every 24 h for up to 4 days.

Liquid chromatography–mass spectrometry (LC-MS) analysis of *Collimonas diffusates*

Diffusates were diluted 10x in 100% LC-MS grade methanol, filtered over a 0.22 μm membrane and injected (5 μl) into a Thermo UltiMate 3000 UHPLC system equipped with a Thermo Q Exactive Hybrid Quadrupole-Orbitrap Mass Spectrometer (LC-HESI-HiRes MS). The column used for the separation was an Agilent ZORBAX RRHD Eclipse Plus C18 (2.1 X 150mm, 1.8 μm , 959759-902). The gradient elution involved a mobile phase consisting of (A) 0.1% formic acid in water and (B) 0.1% formic acid in acetonitrile. The initial condition was set at 5%-B for 1.0 min. A linear gradient to 95%-B was applied in 12 min followed by another 5 min of gradient to 100%-B. The gradient was then returned to starting conditions and held for 7 min. Flow rate was set at 0.3 ml/min. The electrospray ionization mass spectra were acquired in both positive and negative ion mode. Mass data were collected between $m/z = 133$ and 2,000. The ion spray voltage was set at 3,500V; gas temperature and auxiliary gas temperature were maintained at 380°C and 425°C respectively. The sheath gas flow and auxiliary gas flow were set at 60 and 20 arbitrary units respectively. Sample analysis was performed using Progenesis with an intensity cut-off of 800. Compound identification was done with Chemspider, using BioCyc, KEGG, ChEBI, peptides, ChemBank, MassBank, Natural Products Updates, Nature Chemical Biology, Nature Chemistry, NIST, PlantCyc, PubMed and Wikidata as data sources.

Greenhouse experiments

To test the ability of CaCal35 and its mutant derivatives to protect tomato plants from *Fol*, we performed a greenhouse experiment as described before (Doan *et al.*, 2020). Briefly, tomato seedlings (Early Pak 7) were grown from surface-sterilized seed in UC potting soil mix for 11–15 days (two true leaves), at which point whole plants were extracted from the soil and their roots dipped for five min in one of the following suspensions (in water): water only (control, no bacteria), CaCal35 (10^6 cells/ml), BvFZB42 (10^6 spores/ml), a 1:1 mixture of CaCal35 (10^6 cells/ml) and BvFZB42 (10^6 spores/ml) suspensions (we refer to this mixture as *Collii42*), a 1:1 mixture of CaCal35 (10^6 cells/ml) and AK3 (10^6 spores/ml), a 1:1 mixture of BvFZB42 (10^6 spores/ml) and 46A06 (10^6 cells/ml), or a 1:1 mixture of BvFZB42 (10^6 spores/ml) and 60C09 (10^6 cells/ml), before transfer to pots containing fresh UC potting soil mix. One week

later, plants and their roots were again recovered from the soil, and roots were dipped for five min in either water (no-*Fol* control) or a *Fol* spore suspension in water (10^6 spores/ml), prepared as before (Doan *et al.*, 2020) and transplanted to individual pots containing fresh UC potting soil mix. After three days, the soil around the crown of individual plants was drenched by pouring onto the soil surface 100 ml of water, or 100 ml of the same bacterial suspension that the roots of the plant had originally been dipped into. One week later, this drench was repeated. The plants received supplemental fertilization every day or every other day (all values in ppm: N 144.1, P 63.707, K 204.8, Ca 119.1, Mg 49.467, S 65.114, Fe 2.759, Cu 0.097, B 0.4, Mn 0.633, Mo 0.055 and Zn 0.097) through the irrigation system of the greenhouse.

Per treatment (of which there were eight: no-*Fol*, no bacteria; *Fol*-only, no bacteria; *Fol* plus *CaCal35* only; *Fol* plus *BvFZB42* only; *Fol* plus *CaCal35* and *BvFZB42* (i.e. *Colli42*); *Fol* plus *CaCal35* and AK3; *Fol* plus 46A06 and *BvFZB42*; *Fol* plus 46A06 and AK3), we used ten plants which were organized in a random block design in the greenhouse. Five weeks after *Fol* inoculation (i.e. at the onset of flowering), all ten tomato plants per treatment were assessed for vascular discoloration and shoot dry weight. Discoloration was measured as before (Doan *et al.*, 2020) on a scale from 0 to 4 (0, no vascular discoloration; 1, <5% discoloration, typically light brown; 2, 5–20% discoloration, typically light brown; 3, 20–40% discoloration, typically dark brown; 4, >40% discoloration, typically dark brown). Shoots were dried at 65°C for 1 week before weighing.

The experiment was performed four independent times to compare the no-*Fol*, *Fol*-only, *Fol* plus *CaCal35*, *Fol* plus *BvFZB42* and plus *Colli42* treatments, and three independent times to compare the no-*Fol*, *Fol*-only, *Fol* plus *Colli42*, *Fol* plus *CaCal35* and AK3, *Fol* plus 46A06 and *BvFZB42*, and *Fol* plus 46A06 and AK3 treatments. For each one of the independent experiments, relative shoot biomass was calculated for each treatment as $(a-b)/(c-b) \times 100\%$, where *a* is the shoot dry weight averaged for all ten plants of a particular treatment, *b* is the shoot dry weight averaged for all ten plants in the *Fol*-only treatment, and *c* is the dry weight averaged for all ten plants in the no-*Fol* treatment. Differences in relative biomass and in vascular discoloration between treatments across replicated experiments were statistically assessed using analysis of variance (ANOVA) with multiple comparisons using Tukey–Kramer test ($P < 0.05$).

Field trial

A field trial with *Colli42* was carried out at the Armstrong Plant Pathology Field Station at UC Davis. This field

was artificially infested with the tomato wilt pathogen *Fol*, race 3 in previous years (Doan *et al.*, 2020). Tomato plants (Heinz 8504; VFFN, i.e. resistant to *Fol* race 1 and 2 but not race 3, and also resistant to *V. dahliae* race 1 and root knot nematode) were seeded in seedling trays with 3.5 x 3.5 x 6.5 cm cells and kept in the greenhouse for 3 weeks, at which time individual trays were dipped in one of the following bacterial suspensions (prepared and with cell densities as described in the section ‘Greenhouse experiments’): (i) no cells (i.e. water), (ii) *CaCal35*, (iii) *BvFZB42* or (iv) *Colli42*. Dipped trays were placed back in the greenhouse and after 1 week (on May 14, 2018), tomato seedlings were transplanted at 30 cm apart into a drip-irrigated plot with a randomized complete block design (single-row 92-cm beds with 60-cm between-row spacing beds, plus a pair of border rows; 30 plants per bed, four beds per treatment) featuring four blocks with four beds per block. After 1 week, 10 litres of water or a suspension of *CaCal35*, *BvFZB42* or *Colli42* (prepared as before) was drip-delivered into each one of the corresponding blocks. One week later, this delivery was repeated. The field was drip-irrigated as needed. Fertilizer UN-32 (16.5% urea N, 7.75% nitrate N and 7.75% ammoniacal N) was applied through the drip once a week until flowering, at 75 ml per block and starting 12 days after transplanting. All plants also received a one-time application of Miracle-Gro Quick Start (Scotts Miracle-Gro, Marysville, OH) 5 days after transplanting, at 450 ml per block. Weeding was done manually, and no herbicides or pesticides were used. Fruits were harvested on 19 September 2018 (4 months after planting), at which time more than 90 per cent of the fruit were ripe. Vascular discoloration (same scaling as for the greenhouse experiment) was determined and averaged for each one of 15 plants in the centre of each bed, as described above. Also determined for these 15 plants combined were the weights of red (marketable) tomato fruit. Marketable yield was calculated and expressed in tons per acre. Differences in yield and vascular discoloration between treatments were determined using analysis of variance (ANOVA) with multiple comparisons using Tukey–Kramer test ($P < 0.05$).

Acknowledgements

Research reported here was supported by Novozymes North America, Inc. JHJL and HKD are both listed as inventors on patent # US 9,485,994 B2 (issued 8 November 2016) which is entitled ‘Synergy-based bio-control of plant pathogens’ and based on previously published work on *Collimonas-Bacillus*-based suppression of plant disease (Doan *et al.*, 2020).

Conflict of interest

None declared.

References

- Bisutti, I.L., and Stephan, D. (2011). *Einsatz mikrobiologischer Präparate zur Regulierung von Schadinsekten und Krankheiten an Erdbeeren* [WWW document].
- Blanco, G., Patallo, E.P., Braña, A.F., Trefzer, A., Bechtold, A., Rohr, J., *et al.* (2001) Identification of a sugar flexible glycosyltransferase from *Streptomyces olivaceus*, the producer of the antitumor polyketide elloramycin. *Chem Biol* **8**: 253–263.
- Borriss, R. (2011) Use of plant-associated *Bacillus* strains as biofertilizers and biocontrol agents in agriculture. In *Bacteria in Agrobiotechnology: Plant Growth Responses*. Maheshwari, D. K. (ed). Berlin: Springer, pp. 41–76.
- Bos, C.J., Debets, A.J., Swart, K., Huybers, A., Kobus, G., and Slakhorst, S.M. (1988) Genetic analysis and the construction of master strains for assignment of genes to six linkage groups in *Aspergillus niger*. *Curr Genet* **14**: 437–443.
- Breukink, E., and de Kruijff, B. (2006) Lipid II as a target for antibiotics. *Nat Rev Drug Discovery* **5**: 321–332.
- Chen, Y.L., Chen, Y.H., Lin, Y.C., Tsai, K.C., and Chiu, H.T. (2009) Functional characterization and substrate specificity of spinosyn rhamnosyltransferase by in vitro reconstitution of spinosyn biosynthetic enzymes. *J Biol Chem* **284**: 7352–7363.
- Chen, X.H., Koumoutsis, A., Scholz, R., Eisenreich, A., Schneider, K., Heinemeyer, I., *et al.* (2007) Comparative analysis of the complete genome sequence of the plant growth-promoting bacterium *Bacillus amyloliquefaciens* FZB42. *Nat Biotechnol* **25**: 1007–1014.
- Chowdhury, S.P., Dietel, K., Rändler, M., Schmid, M., Junge, H., Borriss, R., *et al.* (2013) Effects of *Bacillus amyloliquefaciens* FZB42 on lettuce growth and health under pathogen pressure and its impact on the rhizosphere bacterial community. *PLoS One* **8**: e68818.
- Chowdhury, S.P., Hartmann, A., Gao, X.W., and Borriss, R. (2015a) Biocontrol mechanism by root-associated *Bacillus amyloliquefaciens* FZB42—a review. *Front Microbiol* **6**: 780.
- Chowdhury, S.P., Uhl, J., Grosch, R., Alquéres, S., Pittroff, S., Dietel, K., *et al.* (2015b) Cyclic lipopeptides of *Bacillus amyloliquefaciens* subsp. *plantarum* colonizing the lettuce rhizosphere enhance plant defense responses toward the bottom rot pathogen *Rhizoctonia solani*. *Mol Plant Microbe Interact* **28**: 984–995.
- Doan, H.K., and Davis, R.M. (2014) Evaluation of fusarium wilt resistance in six upland cotton germplasm lines. *J Cotton Sci* **18**: 430–434.
- Doan, H.K., Maharaj, N.N., Kelly, K.N., Miyao, E.M., Davis, R.M., and Leveau, J.H.J. (2020) Antimycotal activity of *Collimonas* isolates and synergy-based biological control of Fusarium wilt of tomato. *Phytobiomes J* **4**: 64–74.
- Dunlap, C.A., Kim, S.J., Kwon, S.W., and Rooney, A.P. (2016) *Bacillus velezensis* is not a later heterotypic synonym of *Bacillus amyloliquefaciens*; *Bacillus methylophilus*, *Bacillus amyloliquefaciens* subsp. *plantarum* and '*Bacillus oryzae*' are later heterotypic synonyms of *Bacillus velezensis* based on phylogenomics. *Int J Syst Evol Microbiol* **66**: 1212–1217.
- Fan, B., Wang, C., Song, X., Ding, X., Wu, L., Wu, H., *et al.* (2018) *Bacillus velezensis* FZB42 in 2018: the Gram-positive model strain for plant growth promotion and biocontrol. *Front Microbiol* **9**: 2491.
- Fischbach, M.A., and Walsh, C.T. (2006) Assembly-line enzymology for polyketide and nonribosomal peptide antibiotics: logic, machinery, and mechanisms. *Chem Rev* **106**: 3468–3496.
- Fritsche, K., van den Berg, M., de Boer, W., van Beek, T.A., Raaijmakers, J.M., van Veen, J. A., and Leveau, J.H.J. (2014) Biosynthetic genes and activity spectrum of antifungal polyynes from *Collimonas fungivorans* Ter331. *Environ Microbiol* **16**: 1334–1345.
- Fujinami, S., and Ito, M. (2018) The surface layer homology domain-containing proteins of alkaliphilic *Bacillus pseudofirmus* OF4 play an important role in alkaline adaptation via peptidoglycan synthesis. *Front Microbiol* **9**: 810.
- Greule, A., Intra, B., Flemming, S., Rommel, M.G.E., Panbangred, W., and Bechtold, A. (2016) The draft genome sequence of *Actinokineospora bangkokensis* 44EHW^T reveals the biosynthetic pathway of the antifungal thalidomide compounds with unusual butylmalonyl-CoA extender units. *Molecules* **21**: 1607.
- Gül, A., Kidoglu, F., and Tüzel, Y. (2008) Effects of nutrition and *Bacillus amyloliquefaciens* on tomato (*Solanum lycopersicum* L.) growing in perlite. *Spanish J Agric Res* **6**: 422–429.
- Hager, F.F., López-Guzmán, A., Krauter, S., Blaukopf, M., Polter, M., Brockhausen, I., *et al.* (2018) Functional characterization of enzymatic steps involved in pyruvylation of bacterial secondary cell wall polymer fragments. *Front Microbiol* **9**: 1356.
- Hager, F.F., Sützl, L., Stefanovic, C., Blaukopf, M., and Schäffer, C. (2019) Pyruvate substitutions on glycoconjugates. *Int J Mol Sci* **20**: 4929.
- Horsman, M.E., Marous, D.R., Li, R., Oliver, R.A., Byun, B., Emrich, S.J., *et al.* (2017) Whole-genome shotgun sequencing of two β -proteobacterial species in search of the bulgecin biosynthetic cluster. *ACS Chem Biol* **12**: 2552–2557.
- Ivashina, T.V., Fedorova, E.E., Ashina, N.P., Kalinchuk, N.A., Druzhinina, T.N., Shashkov, A.S., *et al.* (2010) Mutation in the *pssM* gene encoding ketal pyruvate transferase leads to disruption of *Rhizobium leguminosarum* bv. *viciae*-*Pisum sativum* symbiosis. *J Appl Microbiol* **109**: 731–742.
- Kai, K., Sogame, M., Sakurai, F., Nasu, N., and Fujita, M. (2018) Collimonins A-D, unstable polyynes with antifungal or pigmentation activities from the fungus-feeding bacterium *Collimonas fungivorans* Ter331. *Org Lett* **20**: 3536–3540.
- Kalynych, S., Morona, R., and Cygler, M. (2014) Progress in understanding the assembly process of bacterial O-antigen. *FEMS Microbiol Rev* **38**: 1048–1065.
- Kamilova, F., Leveau, J.H.J., and Lugtenberg, B. (2007) *Collimonas fungivorans*, an unpredicted *in vitro* but efficient *in vivo* biocontrol agent for the suppression of tomato foot and root rot. *Environ Microbiol* **9**: 1597–1603.

- Kaysser, L., Wemakor, E., Siebenberg, S., Salas, J.A., Sohng, J.K., Kammerer, B., and Gust, B. (2010) Formation and attachment of the deoxysugar moiety and assembly of the gene cluster for caprazamycin biosynthesis. *Appl Environ Microbiol* **76**: 4008–4018.
- Kenyon, J.J., Shashkov, A.S., Senchenkova, S.N., Shneider, M.M., Liu, B., Popova, A.V., *et al.* (2017) *Acinetobacter baumannii* K11 and K83 capsular polysaccharides have the same 6-deoxy-L-talose-containing pentasaccharide K units but different linkages between the K units. *Int J Biol Macromol* **103**: 648–655.
- Kim, B.Y., Weon, H.Y., Yoo, S.H., Chen, W.M., Kwon, S.W., Go, S.J., and Stackebrandt, E. (2006) *Chitinimonas koreensis* sp. nov., isolated from greenhouse soil in Korea. *Int J Syst Evol Microbiol* **56**: 1761–1764.
- King, J.D., Kocincova, D., Westman, E.L., and Lam, J.S. (2009) Lipopolysaccharide biosynthesis in *Pseudomonas aeruginosa*. *Innate Immunity* **15**: 261–312.
- Koumoutsis, A., Chen, X.-H., Henne, A., Liesegang, H., Hitzeroth, G., Franke, P., *et al.* (2004) Structural and functional characterization of gene clusters directing nonribosomal synthesis of bioactive cyclic lipopeptides in *Bacillus amyloliquefaciens* strain FZB42. *J Bacteriol* **186**: 1084–1096.
- de Kruijff, B., van Dam, V., and Breukink, E. (2008) Lipid II: a central component in bacterial cell wall synthesis and a target for antibiotics. *Prostaglandins Leukot Essent Fatty Acids* **79**: 117–121.
- Leveau, J.H.J., Uroz, S., and de Boer, W. (2010) The bacterial genus *Collimonas*: mycophagy, weathering and other adaptive solutions to life in oligotrophic soil environments. *Environ Microbiol* **12**: 281–292.
- Manker, D.C. (2004) Natural products as green pesticides. In *New discoveries in agrochemicals*. Clark, J.M., and Ohkawa, H. (eds). Washington, DC: American Chemical Society, pp. 283–294.
- Marrone, P.G. (2002) An effective biofungicide with novel modes of action. *Pestic Outlook* **13**: 193–194.
- Medema, M.H., Blin, K., Cimermancic, P., de Jager, V., Zakrzewski, P., Fischbach, M.A., *et al.* (2011) anti-SMASH: rapid identification, annotation and analysis of secondary metabolite biosynthesis gene clusters in bacterial and fungal genome sequences. *Nucleic Acids Res* **39**: 339–346.
- Mela, F., Fritsche, K., de Boer, W., van den Berg, M., van Veen, J.A., Maharaj, N.N., and Leveau, J.H.J. (2012) Comparative genomics of bacteria from the genus *Collimonas*: linking (dis)similarities in gene content to phenotypic variation and conservation. *Environ Microbiol Rep* **4**: 424–432.
- Mela, F., Fritsche, K., de Boer, W., van Veen, J.A., de Graaff, L.H., van den Berg, M., and Leveau, J.H.J. (2011) Dual transcriptional profiling of a bacterial/fungal confrontation: *Collimonas fungivorans* versus *Aspergillus niger*. *ISME J* **5**: 1494–1504.
- Morona, R., Macpherson, D.F., Vandenbosch, L., Carlin, N.I.A., and Manning, P.A. (1995) Lipopolysaccharide with an altered O-antigen produced in *Escherichia coli* K-12 harboring mutated, cloned *Shigella flexneri* *rfb* Genes. *Mol Microbiol* **18**: 209–223.
- Mosquera, S., Stergiopoulos, I., and Leveau, J.H.J. (2020) Interruption of *Aspergillus niger* spore germination by the bacterially produced secondary metabolite collimomycin. *Environ Microbiol Rep* **12**: 306–313.
- Muldowney, M.W., McClure, R.A., Robey, M.T., Kelleher, N.L., and Thomson, R.J. (2018) Natural products from thioester reductase containing biosynthetic pathways. *Nat Product Rep* **35**: 847–878.
- Neuhof, T., Schmieder, P., Seibold, M., Preussel, K., and von Döhren, H. (2006) Hassallidin B - second antifungal member of the hassallidin family. *Bioorg Med Chem Lett* **16**: 4220–4222.
- Opelt, K., and Berg, G. (2004) Diversity and antagonistic potential of bacteria associated with bryophytes from nutrient-poor habitats of the Baltic Sea coast. *Appl Environ Microbiol* **70**: 6569–6579.
- Pan, Y.-J., Lin, T.-L., Chen, C.-T., Chen, Y.-Y., Hsieh, P.-F., Hsu, C.-R., *et al.* (2015) Genetic analysis of capsular polysaccharide synthesis gene clusters in 79 capsular types of *Klebsiella* spp. *Sci Rep* **5**: 15573.
- Parker, W.L., Rathnum, M.L., Johnson, J.H., Wells, J.S., Principe, P.A., and Sykes, R.B. (1988) Aerocyanidin, a new antibiotic produced by *Chromobacterium violaceum*. *J Antibiot* **41**: 454–460.
- Patiny, L., and Borel, A. (2013) ChemCalc: a building block for tomorrow's chemical infrastructure. *J Chem Inf Model* **53**: 1223–1228.
- Qiao, K.J., Zhou, H., Xu, W., Zhang, W.J., Garg, N., and Tang, Y. (2011) A fungal nonribosomal peptide synthetase module that can synthesize thiopyrazines. *Org Lett* **13**: 1758–1761.
- Rausch, C., Weber, T., Kohlbacher, O., Wohlleben, W., and Huson, D.H. (2005) Specificity prediction of adenylation domains in nonribosomal peptide synthetases (NRPS) using transductive support vector machines (TSVMs). *Nucleic Acids Res* **33**: 5799–5808.
- Sambrook, J., and Russel, D.W. (2001) *Molecular cloning, a laboratory manual*. Cold Spring Harbor, New York: Cold Spring Harbor Laboratory Press.
- Schmidt, Y., van der Voort, M., Crusemann, M., Piel, J., Josten, M., Sahl, H.G., *et al.* (2014) Biosynthetic origin of the antibiotic cyclocarbamate brabantamide A (SB-253514) in plant-associated *Pseudomonas*. *ChemBioChem* **15**: 259–266.
- Scott, P.M., Erickson, K.M., and Troutman, J.M. (2019) Identification of the functional roles of six key proteins in the biosynthesis of Enterobacteriaceae colanic acid. *Biochemistry* **58**: 1818–1830.
- Singh, P.D., Liu, W.-C., Gougoutas, J.Z., Malley, M.F., Porubcan, M.A., Trejo, W.H., *et al.* (1988) Aerocavin, a new antibiotic produced by *Chromobacterium violaceum*. *J Antibiot* **41**: 446–453.
- Solovyev, V., and Salamov, A. (2011) Automatic annotation of microbial genomes and metagenomic sequences. In *Metagenomics and its Applications in Agriculture, Biomedicine and Environmental Studies*. Li, R.W. (ed). Hauppauge, NY: Nova Science Publishers, pp. 61–78.
- Song, C., Schmidt, R., de Jager, V., Krzyzanowska, D., Jongedijk, E., Cankar, K., *et al.* (2015) Exploring the genomic traits of fungus-feeding bacterial genus *Collimonas*. *BMC Genom* **16**: 1103.
- Stevenson, G., Andrianopoulos, K., Hobbs, M., and Reeves, P.R. (1996) Organization of the *Escherichia coli*

- K-12 gene cluster responsible for production of the extracellular polysaccharide colanic acid. *J Bacteriol* **178**: 4885–4893.
- Sylla, J., Wohanka, W., and Krüger-Steden, E. (2012). *Ein-satz mikrobiologischer Präparate zur Regulierung von Krankheiten an Erdbeeren - Teilprojekt: Graufäule und Echter Mehltau* [WWW document].
- Tecon, R., and Leveau, J.H.J. (2016) Symplasmata are a clonal, conditional, and reversible type of bacterial multicellularity. *Sci Rep* **6**: 31914.
- Uroz, S., Tech, J.J., Sawaya, N.A., Frey-Klett, P., and Leveau, J.H.J. (2014) Structure and function of bacterial communities in ageing soils: Insights from the Mendocino ecological staircase. *Soil Biol Biochem* **69**: 265–274.
- Vandamme, P., Opelt, K., Knöchel, N., Berg, C., Schönmann, S., De Brandt, E., *et al.* (2007) *Burkholderia bryophila* sp nov and *Burkholderia megapolitana* sp nov., moss-associated species with antifungal and plant-growth-promoting properties. *Int J Syst Evol Microbiol* **57**: 2228–2235.
- Wang, X.L., Yang, F., and von Bodman, S.B. (2012) The genetic and structural basis of two distinct terminal side branch residues in stewartan and amylovoran exopolysaccharides and their potential role in host adaptation. *Mol Microbiol* **83**: 195–207.
- Wu, J.J., de Jager, V.C., Deng, W.L., and Leveau, J.H.J. (2015) Finished genome sequence of *Collimonas arenae* Cal35. *Genome Announc* **3**: e01408–01414.
- Yao, A.V., Bochow, H., Karimov, S., Boturov, U., Sangin-boy, S., and Sharipov, A.K. (2006) Effect of FZB 24® *Bacillus subtilis* as a biofertilizer on cotton yields in field tests. *Arch Phytopathol* **39**: 323–328.

Supporting information

Additional supporting information may be found online in the Supporting Information section at the end of the article.

Fig. S1. Photographs of tomato plants from a representative greenhouse experiment showing the protective effect of *Colli42*, i.e. a mixture of *CaCal35* and *BvFZB42*, against *Fol* (panel D). Other panels: A, unchallenged plants (no-*Fol*); B, untreated, *Fol*-challenged plants (*Fol*-only); C, *CaCal35*-treated, *Fol*-challenged plants; and E, *BvFZB42*-treated, *Fol*-challenged plants. Note the inability of *CaCal35* and *BvFZB42* to protect plants from *Fol*.

Fig. S2. Identification of two transposon mutants of *CaCal35*, i.e. 46A06 and 60C09, with reduced antifungal

activity. Shown are two 96-well, bottomless microtitre plates, where each well containing 250 μ l PDA was inoculated from the top with 3 μ l of a 10^5 spores/ml *A. niger* spore suspension and from the bottom with one of 6,500 *CaCal35* transposon insertion mutants. Plates were incubated at 28°C for 48 h and photographed from the top. Fungal growth was observed only on plate 46, row A, column 6 (left panel), which identified mutant 46A06 (left panel), while mutant 60C09 (right panel) was identified on plate 60, row C, column 9. The coloration in some of the other wells does not represent fungal growth on top of the PDA, but rather bacterial biomass on the bottom side.

Fig. S3. Transposon insertion sites for *CaCal35* mutants 46A06 (panels A–C) and 60C09 (panels D–F). Shown for both mutants are the sequencing chromatograms generated by primer KAN-2FP1 (panels A and D) or KAN-2RP1 (panels B and E), and annotated (by underline) with the location of 19-bp mosaic ends and 9-bp insertion sites. Also shown (panels C and F) are the DNA sequences flanking the insertion sites (in red) for both mutants on the *CaCal35* genome.

Fig. S4. Comparison of the *CaCal35* genomic region identified through mutant 46A06 mutant to genomic regions *Chromobacterium violaceum* ATCC 53434, *Chitinimonas koreensis* DSM 17726, and *Paraburkholderia megapolitana* LMG 23650. Not shown is the corresponding genomic region of *Paraburkholderia acidophila* ATCC 31363, which is similar to that of *P. megapolitana* LMG 23650. Points of reference for the *CaCal35* genomic region are genes LT85_RS01600 and LT85_RS01800 which are the first and last genes, respectively, listed in Table S1. Only the coloured genes in all of the other genomic regions represent genes with homologues in the *CaCal35* genomic region; for the predicted products of those genes, amino acid sequence identity (in %) to that of the corresponding gene product in *CaCal35* is shown. On the *CaCal35* genomic region, starting with LT85_RS01720, eleven genes are labelled as belonging to the *cpl* (for carenaemin production locus) gene cluster. The black triangle indicates the location of the transposon insertion in 46A06 in LT85_RS01670 (i.e. *cplI*).

Fig. S5. Method for collection of diffusates from wild-type *CaCal35* and mutants 46A06 and 60C09. Shown are representative PDA plates with wells in the agar (10 wells per plate) which were previously filled with PDB to allow recovery by diffusion of metabolites produced by the bacterial biomass growing on the agar surrounding the wells. See text for more details.

Table S1. BlastP analysis of predicted Cpl proteins encoded by the *cpl* gene cluster.